Substitution of the Carboxyl-terminal Domain of apo AI with apo AII Sequences Restores the Potential of HDL to Reduce the Progression of Atherosclerosis in apo E Knockout Mice

Paul Holvoet, Sophie Danloy, Els Deridder, Marleen Lox, Hilde Bernar, Ann Dhoest, and Désiré Collen
Center for Molecular and Vascular Biology, University of Leuven, Leuven, Belgium

Abstract

HDL metabolism and atherosclerosis were studied in apo E knockout (KO) mice overexpressing human apo AI, a des-(190-243)-apo AI carboxyl-terminal deletion mutant of human apo AI or an apo AI-(1-189)-apo AII-(12-77) chimera in which the carboxyl-terminal domain of apo AI was substituted with the pair of helices of apo AII. HDL cholesterol levels ranked: apo AI/apo E KO ∼ apo AI-(1-189)-apo AII-(12-77)/apo E KO > > des-(190-243)-apo AI/apo E KO > apo E KO mice. Progression of atherosclerosis ranked: apo E KO > des-(190-243)-apo AI/apo E KO > > apo AI-(1-189)-apo AII-(12-77)/apo E KO ∼ apo AI/apo E KO mice. Whereas the total capacity to induce cholesterol efflux from lipid-loaded THP-1 macrophages was higher for HDL of mice overexpressing human apo AI or the apo AI/apo AII chimera, the fractional cholesterol efflux rate, expressed in percent cholesterol efflux/μg apolipoprotein/h, for HDL of these mice was similar to that for HDL of mice overexpressing the deletion mutant and for HDL of apo E KO mice. This study demonstrates that the tertiary structure of apo AI, e.g., the number and organization of its helices, and not its amino sequence is essential for protection against atherosclerosis because it determines HDL cholesterol levels and not cholesterol efflux. Amino acid sequences of apo AII, which is considered to be less antiatherogenic, can be used to restore the structure of apo AI and thereby its antiatherogenicity. (*J. Clin. Invest.* 1998. 102:379–385.) Key words: atherosclerosis • transgenic mice • apo AI • apo AII • reverse cholesterol transport

Introduction

Low plasma levels of HDL and of their major component, apo AI, correlate with an increased risk for coronary heart disease (1). apo AI, the major protein component of HDL, is an important determinant of the concentration of HDL in human blood (2, 3). Overexpression of human apo AI in transgenic mice resulted in increased plasma levels of small HDL particles comparable to human HDL_3 (4–6). HDL cholesterol levels and human apo AI levels were highly correlated and dietary fat increased HDL levels in these mice both by increasing the transport rates and decreasing the fractional catabolic rates of HDL cholesterol ester and apo AI (4–7). Overexpression of human apo AI in the atherosclerosis susceptible C57BL/6J mouse strain resulted in a sevenfold reduction of lesion areas in the aorta (8). Introduction of the human apo AI transgene in apo E knockout (KO)[1] mice, characterized by very high levels of proatherogenic βVLDL and accelerated progression of complex atherosclerotic lesions (9–12), resulted in a significant protection against atherosclerosis (13, 14). Transgenic mice overexpressing mouse apo AII had increased HDL cholesterol levels, but, nevertheless, exhibited increased diet-induced atherosclerotic lesion development as compared with control mice (15). The concentration of HDL cholesterol in transgenic mice overexpressing human apo AII was lower than in control mice, probably due to the production of small HDL particles that are cleared more rapidly from the circulation, suggesting that sequence differences between human and murine apo AII may affect HDL metabolism (16, 17). Overexpression of human apo AII in human apo AI transgenic mice had no effect on total cholesterol nor on HDL cholesterol but in those apo AII/apo AI transgenic mice lesion areas were 15-fold larger than in apo AI transgenic mice on an atherosclerotic diet (18). These studies demonstrated opposite effects of apo AI and apo AII on atherosclerosis in transgenic mice. However, it is not clear yet whether these opposite effects of apo AI and apo AII depend on differences in their molecular structure, such as number and organization of helices, that may affect HDL metabolism or on differences in amino acid sequence that may affect interaction with peripheral, lipid-loaded foam cells and thereby the reverse cholesterol transport.

Recently, we produced an apo AI-(1-189)-apo AII-(12-77) chimera in which the carboxyl-terminal domain of apo AI was substituted with the pair of helices of apo AII (6). Although the carboxyl-terminal domain of the chimera contained 80% of the amino acid sequence of apo AII, the distribution of amphipathic helices in the chimera was identical to that in human apo AI (19) and overexpression of the human apo AI/apo AII chimera in C57BL/6J mice resulted in a similar increase of HDL cholesterol levels as in mice overexpressing human apo AI (6). In contrast, overexpression of a des-(190-243)-apo AI carboxyl-terminal deletion mutant of human apo AI resulted only in a slight increase of HDL cholesterol levels. Therefore, these mice are well suited to investigate (*a*) whether the car-

Address correspondence to Paul Holvoet, Center for Molecular and Vascular Biology, University of Leuven, Campus Gasthuisberg, O & N, Herestraat 49, B-3000 Leuven, Belgium. Phone: 32-16-345798; FAX: 32-16-345990; E-mail: paul.holvoet@med.kuleuven.ac.be

Received for publication 7 February 1998 and accepted in revised form 8 May 1998.

J. Clin. Invest.

0021-9738/98/07/0379/07 $2.00
Volume 102, Number 2, July 1998, 379–385
http://www.jci.org

1. *Abbreviations used in this paper:* apo AI-(1-189)-apo AII-(12-77), chimera containing the Asp1-Leu189 segment of apo AI linked to the Ser12-Gln77 segment of apo AII; des-(190-243)-apo AI, apo AI mutant with deletion of the Ala190-Gln243 segment; KO, knockout.

boxyl-terminal domain of apo AI is essential for the antiatherogenic properties of HDL independent of the role of the domain in the association of apo AI to lipoprotein particles; and (*b*) whether insertion of helices of apo AII in the apo AI structure affects the potential of HDL to induce cholesterol efflux and to reduce the progression of atherosclerosis independent of HDL cholesterol levels.

Methods

Animal experiments. All experimental procedures in animals were performed in accordance with protocols approved by the Institutional Animal Care and Research Advisory Committee. Transgenic mice that overexpress human apo AI, a human des-(190-243)-apo AI deletion mutant, and a human apo AI-(1-189)-apo AII-(12-77) chimera were generated by zygote injection into the C57BL/6J background, as described previously (6). Mice with inactivated apo E genes, apo E KO mice (10), backcrossed for 10 generations into the C57BL/6J background, were purchased from The Jackson Laboratory (Bar Harbor, ME). These mice had 98.4% C57BL/6J background. Males homozygous for the transgene were mated with apo E KO females and double homozygous offspring (third generation) were used. Mice were fed normal chow ad libitum.

Apolipoprotein quantitation by ELISA and Western blotting. Blood was collected in heparinized microhematocrit capillary tubes from the tail or from the retroorbital plexus. After centrifugation (2,000 *g* for 5 min), human apo AI variants were quantitated by a sandwich ELISA using murine monoclonal antibodies directed against human apo AI as described previously (6). The antibodies used in this assay had $< 0.01\%$ cross-reactivity with murine apo AI. Recombinant apo AI, des-(190-243)-apo AI, and apo AI-(1-189)-apo AII-(12-77) were purified from the periplasmic fraction of *Escherichia coli* cells as previously described (19) and purified proteins were used as standards in the ELISA. The lower limit of sensitivity of the ELISA was similar (5 ng/ml in 200-fold diluted plasma) for all apo AI variants. The interassay variation coefficient of the ELISA was 12%. Alternatively, levels of human apo AI were determined by quantitative scanning of Western immunoblots of 10–15% gradient SDS-polyacrylamide gels that had been developed with the monoclonal antibodies against human apo AI. For quantitation of murine apo AI, Western immunoblots were developed with polyclonal anti–mouse apo AI antibodies prepared in cynomolgus monkeys and generously supplied by Dr. George Melchior (Upjohn, Kalamazoo, MI). These antibodies had $< 0.01\%$ cross-reactivity with human apo AI. The interassay variation coefficient of the immunoblot assay was 20%.

Plasma lipoprotein analyses. Mice were fasted overnight and blood was drawn from the retroorbital plexus into EDTA tubes. Plasma was obtained by centrifugation and lipoprotein fractions were separated by gel filtration on a Superdex 200 HR column equilibrated with 20 mM Tris-HCl buffer, pH 8.1, containing 0.15 M NaCl, 1 mM EDTA, and 0.02 mg/ml sodium azide in a FPLC system (Waters Associates, Milford, MA) (6). 200-μl samples of three mice per group were applied. The plasma levels of phospholipids were determined using standard enzymatic assays (Biomérieux, Marcy, France and Boehringer Mannheim, Meylon, France, respectively) and the protein levels were determined according to Bradford (20). The levels of cholesterol and cholesterol esters in the gel filtration fractions were quantified by HPLC on a Zorbax ODS reversed phase column (6). They were eluted isocratically at 45°C with a mixture of acetonitrile/isopropanol, at ratios of 50:50 and 90:10 (vol/vol), respectively.

HDL particle size distribution was assessed by native PAGE (6). Murine apo AI and human apo AI distribution in HDL was assessed by Western blotting using either polyclonal antibodies raised against murine apo AI or murine monoclonal antibodies raised against human apo AI.

Endogenous apolipoprotein production. Recombinant apo AI, des-(190-243)-apo AI, and apo AI-(1-189)-apo AII-(12-77) were purified from the periplasmic fraction of *E. coli* cells as previously described (19). Proteins were iodinated by the Bolton and Hunter method (21). The specific activities of the different preparations were very similar (7 μCi/μg apolipoprotein). The clearance rates of radiolabeled apolipoproteins were determined in mice as described previously (6). The fractional catabolic rates and the endogenous production rates of the apolipoproteins were calculated from the plasma steady-state concentrations (mg/dl), the clearance rates ($ml \cdot h^{-1}$), and the body weights (g) as described by Kleinberger et al. (22).

Morphometric analysis. Mice were killed and hearts and aortas were fixed in 4% phosphate-buffered formaldehyde and then embedded in 25% gelatin. Quantitative morphometric analysis was performed in a blinded manner using the Leica 2 Quantimet system (Cambridge, England). For each aorta, lesion areas were measured in 16–20 7-μm sections and the mean intimal areas were determined. The first and most proximal section to the heart was taken ~ 100 μm distal to the point were the aorta becomes first rounded (5, 13) and ~ 12 sections per heart were analyzed. Smooth muscle cells and inflammatory cells were detected in an indirect staining procedure using, respectively, a cross-reacting murine monoclonal biotinylated antibody against human smooth muscle cell α-actin (clone 1A4; Sigma Chemical Co., St. Louis, MO; diluted 1:500) or a rat biotinylated monoclonal antibody against murine common leukocyte antigen/CD45 (clone 30F11.1; PharMingen, San Diego, CA; diluted 1:100) and peroxidase-labeled avidin (DAKOPATTS, Copenhagen, Denmark; diluted 1:100). Peroxidase reaction was performed in 0.05 M Tris-HCl (pH 7.0) containing 0.06% 3,3′-diaminobenzidine and 0.01% H_2O_2. Tissue sections were counterstained with hematoxylin. Lipids were stained with oil red O.

Cholesterol efflux assay. Human THP-1 monocytic leukemia cells (23) were obtained from the American Type Culture Collection (Rockville, MD) and maintained in suspension in T-75 culture flasks at a cell density of 2×10^5 to 1×10^6 cells/ml in RPMI 1640 medium containing 10% FCS and 25 μg/ml gentamycin, at 37°C in a 10% CO_2 atmosphere. Cells cultured in the presence of PMA (at a final concentration of 10^{-7} M) were seeded in 35-mm culture dishes (Costar Corp., Cambridge, MA) at a density of 2×10^6 cells/ml and incubated for 24 h. Induction of macrophage differentiation in THP-1 cells was characterized by increased adherence of cells to culture dishes and typical changes in cell morphology. Thereafter, the cells were incubated for 24 h in medium containing 10% lipoprotein-deficient FCS. Cellular uptake and metabolism of unesterified cholesterol and cholesterol esters was evaluated in THP-1–derived macrophages during incubation with malondialdehyde-modified LDL (100 μg/ml) for 16 h as described previously (24). Cholesterol efflux was induced by incubating lipid-loaded THP-1 macrophages with HDL fractions isolated from the plasma of human apo AI/apo E KO, des-(190-243)-apo AI/apo E KO, or apo AI-(1-189)-apo AII-(12-77)/apo E KO mice for 16 h. In a first set of experiments, cells were incubated with the amount of HDL that corresponded to 7.5% of the serum HDL of the respective transgenic mice. In a second set of experiments, cells were incubated with HDL fractions containing 100 μg/ml of the respective apolipoprotein variants.

Statistical analysis. The significance of differences in lipoprotein values and in atherosclerotic lesion areas were tested by a Kruskal-Wallis test followed by a Dunn's multiple comparisons test. $P < 0.05$ was considered statistically significant.

Results

Effects of apo E and apo AI genotype on lipoproteins and apolipoproteins. Total cholesterol levels were very similar in apo E KO ($n = 6$), apo AI/apo E KO ($n = 10$), des-(190-243)-apo AI/apo E KO ($n = 8$), and apo AI-(1-189)-apo AII-(12-77)/apo E KO ($n = 10$) mice (Table I). The predominant lipoprotein class in all these mice was non-HDL cholesterol comprising VLDL and LDL (Fig. 1). The concentration of non-HDL

Table I. Cholesterol (C) and Apolipoprotein Levels in Lipoprotein Fractions Isolated by Gel Filtration of apo E KO, apo AI/apo E KO, des-(190-243)-apo AI/apo E KO, and apo AI-(1-189)-apo AII-(12-77)/apo E KO Mice

Mice	Total C	Non-HDL C	HDL C	Human apo AI	Murine apo AI
	mg/dl	*mg/dl*	*mg/dl*	*mg/dl*	*mg/dl*
apo E KO	620±29	580±25	37±2.3	—	87±6.7
apo AI/apo E KO	705±38	610±30	105±3.5*	240±19	15±1.5*
des-(190-243)-apo AI/apo E KO	600±28	550±26	58±1.7‡§	32±3.4§	81±5.3§
apo AI-(1-189)-apo AII-(12-77)/apo E KO	620±33	540±30	89±2.8*	175±9.8‖	35±2.2*

Data represent mean±SEM. $P \leq 0.001$ vs. apo E KO mice; ‡ $P < 0.01$ vs. apo E KO mice; § $P \leq 0.001$ vs. apo AI/apo E KO mice; ‖ $P \leq 0.01$ vs. apo AI/apo E KO mice.

cholesterol in all these mice was very similar (Table I and Fig. 1). In C57BL/6J mice HDL cholesterol levels were 59±2 mg/dl and non-HDL cholesterol levels were 15±1.0 mg/dl.

HDL cholesterol levels in apo AI/apo E KO, apo AI-(1-189)-apo AII-(12-77)/apo E KO, and in des-(190-243)-apo AI/apo E KO mice were significantly (2.8-, 2.4-, and 1.6-fold, respectively) increased compared with apo E KO mice (Table I and Fig. 1). The ratio of HDL to total cholesterol was 0.060± 0.0037 in apo E KO, 0.15±0.0050 ($P < 0.001$ vs. apo E KO mice) in apo AI/apo E KO, 0.097±0.0058 ($P < 0.01$) in des-(190-243)-apo AI/apo E KO, and 0.14±0.0045 ($P < 0.001$) in apo AI-(1-189)-apo AII-(12-77)/apo E KO mice.

Levels of des-(190-243)-apo AI, measured in ELISA, were 7.5-fold ($P < 0.001$) and 5.5-fold ($P < 0.001$) lower than levels of human apo AI and of apo AI-(1-189)-apo AII-(12-77), respectively (Table I). Levels of murine apo AI were determined by quantitative scanning of Western blots of 10–15% gradient SDS-polyacrylamide gels as described previously (6). Murine apo AI levels were 130±12 mg/dl in C57BL/6J mice and were 1.6-fold lower in apo E KO mice. Compared with murine apo AI levels in apo E KO mice, mean levels were 5.8-fold ($P < 0.001$) lower in apo AI/apo E KO mice, were very similar in des-(190-243)-apo AI/apo E KO mice, and were 2.5-fold ($P < 0.001$) lower in apo AI-(1-189)-apo AII-(12-77)/apo E KO mice (Table I). The ratio of human apo AI to murine apo AI was 16±1.3 in HDL of apo AI/apo E KO, 0.40±0.042 ($P < 0.001$) in HDL of des-(190-243)-apo AI/apo E KO, and 5.0± 0.29 [$P < 0.01$ vs. both HDL of apo AI/apo E KO mice and of des-(190-243)-apo AI/apo E KO mice] in HDL of apo AI-(1-189)-apo AII-(12-77)/apo E KO mice. Total levels of apo AI correlated with the HDL cholesterol levels in apo E KO, apo AI/apo E KO, des-(190-243)-apo AI/apo E KO, and apo AI-(1-189)-apo AII-(12-77)/apo E KO mice ($r = 0.80$; $P < 0.001$; $n = 28$) (data not shown).

More than 85% of lipoprotein-associated apo AI, des-(190-243)-apo AI, or apo AI-(1-189)-apo AII-(12-77) was recovered in the HDL fractions isolated by gel filtration. Nondenaturing gradient PAGE revealed that the HDL of control mice migrated as particles of 9.6 and 7.2 nm, respectively (Fig. 1, *inset*). HDL particles of apo AI/apo E KO and of apo AI-(1-189)-apo AII-(12-77)/apo E KO mice were polydisperse with major populations of particles with diameters of 7.2, 8.4, 9.2, 9.6, and 10.2 nm, respectively (Fig. 1, *inset*). Both human apolipoproteins were distributed over the different HDL particles. Overexpression of des-(190-243)-apo AI resulted in an increase of the smallest HDL particles (Fig. 1, *inset*). Lipoprotein agarose gel electrophoresis revealed that overexpression of human apo AI and of apo AI-(1-189)-apo AII-(12-77) resulted in an increase of lipoprotein particles with α- and preβ-mobility, respectively (data not shown). The electrophoretic pattern of HDL of mice overexpressing the carboxyl-terminal deletion mutant was identical to that of murine HDL which showed α-mobility.

Endogenous apolipoprotein production. Fractional catabolic rates of radiolabeled human apo AI and apo AI-(1-189)-apo AII-(12-77) were very similar, whereas that of des-(190-243)-apo AI was significantly higher (Table II). Endogenous production rates of the different apolipoproteins were calculated from their plasma clearance rates, their steady-state plasma levels, and the body weight of the respective transgenic mice. The values were very similar for all three apo AI variants (Table II).

Effects of apo E and apo AI genotype on atherosclerotic lesion size. Fig. 2 illustrates the sizes of atherosclerotic lesions in the proximal aorta of apo E KO mice at 3, 6, and 9 mo of age,

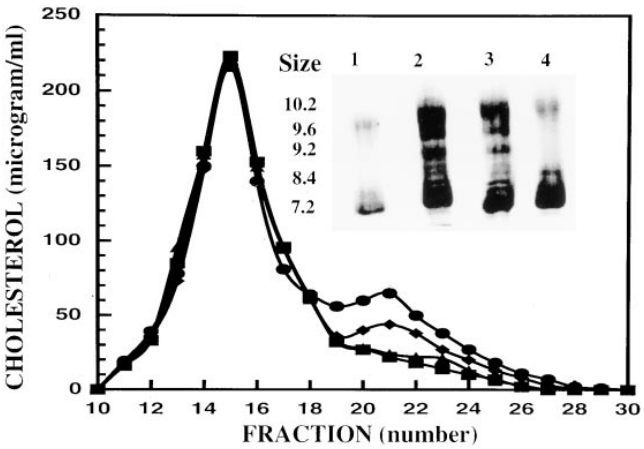

Figure 1. Lipoprotein analysis of mouse plasma by gel filtration. Cholesterol levels in lipoprotein fractions of apo E KO mice (*squares*) and apo E KO mice overexpressing apo AI (*circles*), the apo AI/apo AII chimera (*diamonds*), or the apo AI deletion mutant (*triangles*). Non-HDL cholesterol, containing βVLDL and LDL, were collected in fractions 12–18, whereas HDL cholesterol was collected in fractions 19–25. (*Inset*) Native PAGE of HDL of apo E KO mice (lane *1*), apo E KO mice overexpressing apo AI (lane *2*), the apo AI/apo AII chimera (lane *3*), or the apo AI deletion mutant (lane *4*).

Table II. Apolipoprotein Clearance and Endogenous Apolipoprotein Synthesis in apo AI/apo E KO, des-(190-243)-apo AI/apo E KO, and apo AI-(1-189)-apo AII-(12-77)/apo E KO Mice

Parameter	Apolipoprotein		
	apo AI	des-(190-243)-apo AI	apo AI-(1-189)-apo AII-(12-77)
C_{SS} (mg · dl^{-1})	240±19	32±3.4*	175±9.8‡
FCR (pools · h^{-1})	0.14±0.017	0.63±0.044‡	0.17±0.019
Clp (ml · h^{-1})	0.28±0.029	1.86±0.17*	0.39±0.026‡
PR (mg · h^{-1} · g^{-1})	0.027±0.0022	0.024±0.0025	0.029±0.0032

The data represent mean±SD of three independent experiments. *P* values were determined by Student's *t* test. C_{SS}, steady-state plasma apolipoprotein concentration; *FCR*, fractional catabolic rate; *Clp*, clearance rate; *PR*, endogenous apolipoprotein production rate. $*P \leq 0.001$ vs. human apo AI transgenic mice; $‡P \leq 0.01$ vs. human apo AI transgenic mice.

respectively. Intimal areas increased 18-fold ($P < 0.001$) between 3 and 6 mo and only 1.4-fold (P = NS) between 6 and 9 mo. Therefore, atherosclerotic lesion sizes in transgenic mice were compared at 6 mo. Consistent with previous studies (5, 13), overexpression of human apo AI resulted in a significant reduction of atherosclerotic lesion size (Fig. 2). Overexpression of apo AI-(1-189)-apo AII-(12-77) but not of des-(190-243)-apo AI resulted in a significant reduction of atherosclerotic lesion size and mean intimal areas in apo AI/apo E and apo AI-(1-189)-apo AII-(12-77)/apo E KO mice were similar (Fig. 2).

Fig. 3 illustrates that at 3 mo atherosclerotic lesions in apo E KO mice were fatty streaks consisting of lipid-loaded macrophages (Fig. 3, *A* and *C*). Between 6 and 9 mo, the lesions progressed into fibro-fatty lesions that are similar to advanced human atheromatous plaques (Fig. 3, *B*, *D*, and *E*). These plaques consisted of a fibrous cap containing smooth muscle cells, shoulder areas containing lipid-loaded macrophages, and a necrotic core containing cholesterol crystals (white needle-like structures). Fatty streaks in apo AI/apo E KO mice contained at the most 1–2 layers of macrophage foam cells (*F*). Fatty streaks in apo AI-(1-189)-apo AII-(12-77)/apo E KO (G) and in des-(190-243)-apo AI/apo E KO mice (*H*) were smaller than those in apo E KO mice.

Fig. 4 illustrates that in apo E KO mice overexpressing human apo AI variants HDL cholesterol levels were negatively correlated with mean intimal areas ($r = -0.80$; $n = 28$).

Cholesterol efflux. Cellular cholesterol levels in THP-1–derived macrophages incubated with 100 μg malondialdehyde-

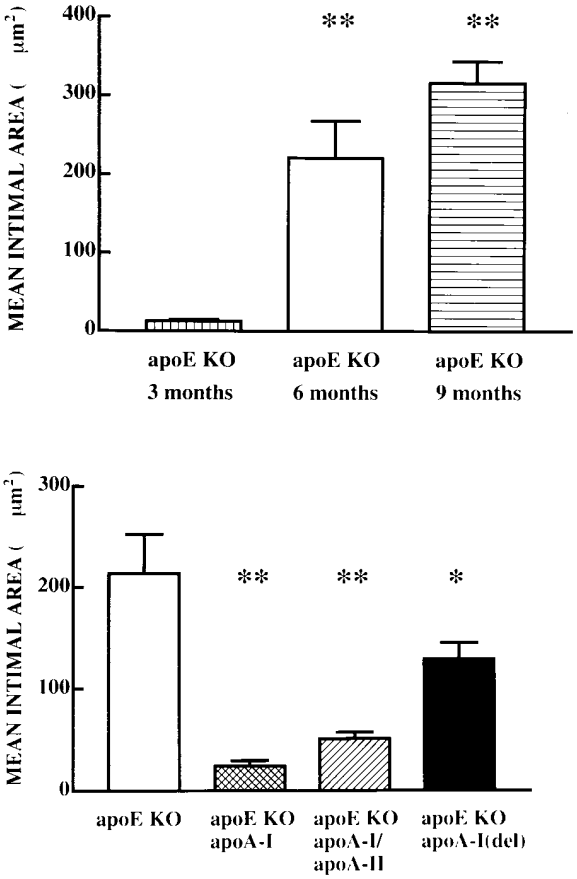

Figure 2. Size of atherosclerotic lesions in aortic segments of apo E KO mice and of apo E KO mice overexpressing human apo AI variants. Mean intimal areas of lesions in aortic segments of apo E KO mice at 3, 6, and 9 mo (*top*) and of apo E KO mice and apo E KO mice overexpressing apo AI, the apo AI/apo AII chimera, or the apo AI deletion mutant at 6 mo (*bottom*).

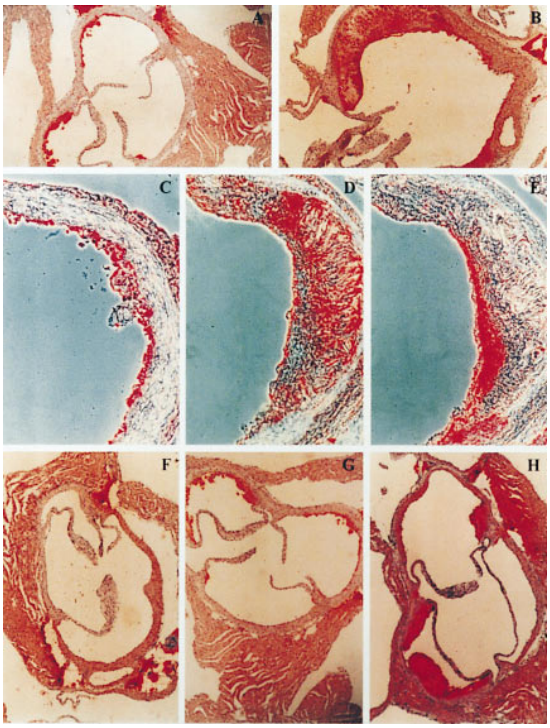

Figure 3. Atherosclerotic lesions in aortic segments of apo E KO mice and of apo E KO mice overexpressing human apo AI variants. Light micrographs (*A* and *B*; ×50) and phase-contrast micrographs (*C–E*; ×200) of aortic segments of apo E KO mice at 3 (*A* and *C*) and 6 mo (*B*, *D*, and *E*), respectively. Lipids in *A* and *B* were stained with oil red O, macrophages (*C* and *D*) were immunostained with the monoclonal antibody 30F11, and smooth muscle cells (*E*) were immunostained with the monoclonal antibody 1A4. Light micrographs of aortic segments of apo E KO mice overexpressing apo AI (*F*), the apo AI/apo AII chimera (*G*), or the apo AI deletion mutant (*H*).

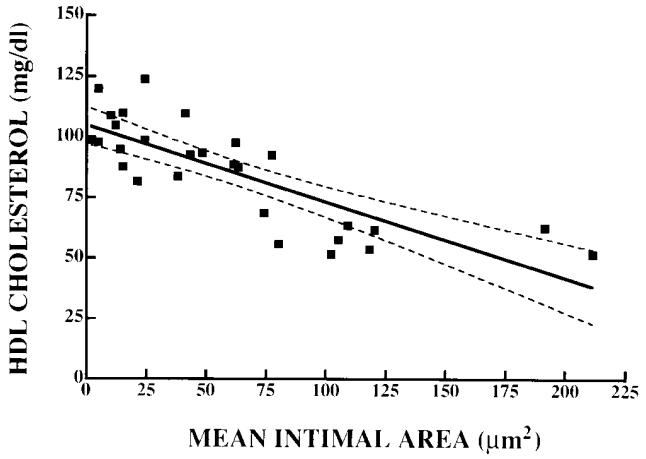

Figure 4. Correlation between HDL cholesterol levels and size of atherosclerotic lesions in aortic segments of apo E KO mice overexpressing apo AI, the apo AI/apo AII chimera, or the apo AI deletion mutant at 6 mo.

modified LDL increased from 25±0.5 μg/mg cell protein (n = 10) to 130±5.1 μg/mg cell protein (n = 10). Incubation of lipid-loaded macrophages with isolated HDL (corresponding to 7.5% of serum HDL) of apo AI/apo E KO and apo AI-(1-189)-apo AII-(12-77)/apo E KO mice resulted in a significant (3.2- and 2.8-fold, respectively) reduction of cellular cholesterol levels. Incubation with HDL of des-(190-243)-apo AI/apo E KO mice resulted in a 1.7-fold reduction of cholesterol levels. However, cholesterol efflux with HDL of des-(190-243)-apo AI/apo E KO mice was not statistically different from that with HDL of apo E KO mice and from that with HDL of C57BL/6J mice (Fig. 5). Cholesterol efflux with HDL of apo AI/apo E KO and with apo AI-(1-189)-apo AII-(12-77)/apo E KO mice was not different from that with HDL of C57BL/6J mice. The fractional rate of cholesterol efflux was 0.032± 0.0021%/μg apolipoprotein/h for HDL of apo AI/apo E KO mice, 0.026±0.0012%/μg apolipoprotein/h for HDL of apo AI-(1-189)-apo AII-(12-77)/apo E KO mice, 0.021± 0.0010%/μg apolipoprotein/h for HDL of des-(190-243)-apo AI/apo E KO mice, 0.021±0.0030%/μg apolipoprotein/h for HDL of apo E KO mice and 0.029±0.0019%/μg apolipoprotein/h for HDL of C57BL/6J mice (Fig. 5).

Discussion

The association between HDL turnover and progression of atherosclerosis was studied in apo E KO mice and apo E KO mice overexpressing human apo AI, a carboxyl-terminal deletion mutant of apo AI or an apo AI/apo AII chimera in which the carboxyl-terminal domain of apo AI was substituted with the helical pairs of apo AII. HDL cholesterol levels in these mice ranked: apo AI/apo E KO ∼ apo AI-(1-189)-apo AII-(12-77)/apo E KO > > des-(190-243)-apo AI/apo E KO > apo E KO mice. The lower HDL cholesterol levels in apo E KO mice overexpressing the carboxyl-terminal deletion mutant were not due to a slower endogenous apolipoprotein production but to the production of smaller HDL particles that were cleared more rapidly from the circulation. As previously observed in C57BL/6J mice (6), overexpression of both human apo AI and of the apo AI/apo AII chimera in apo E KO mice resulted in the appearance of polydisperse HDL particles with a similar distribution profile as human HDL. Therefore, these mice appear to be well suited to investigate whether the carboxyl-terminal domain of apo AI contains sequences that are critical for the antiatherogenic effect of HDL, independent of its contribution to lipoprotein association.

Progression of atherosclerosis ranked: apo E KO > des-(190-243)-apo AI/apo E KO > > apo AI-(1-189)-apo AII-(12-77)/apo E KO ∼ apo AI/apo E KO mice. Because overexpression of the human apo AI variants did not affect the non-HDL cholesterol levels, differences in progression of atherosclerosis could not be ascribed to differences in atherogenic βVLDL cholesterol levels but were most likely due to differences in HDL cholesterol levels. Indeed, HDL cholesterol levels in apo AI/apo E KO, apo AI-(1-189)-apo AII-(12-77)/apo E KO, and des-(190-243)-apo AI/apo E KO mice correlated significantly with the mean intimal areas of atherosclerotic lesions in the proximal aortic segments of these mice. After adjustment for small differences in HDL cholesterol levels in apo AI/apo E KO and apo AI-(1-189)-apo AII-(12-77)/apo E KO mice, the atherosclerosis susceptibility of these mice was very similar.

The antiatherogenic effect of HDL is thought to be linked to its role in the reverse cholesterol transport. This is a process

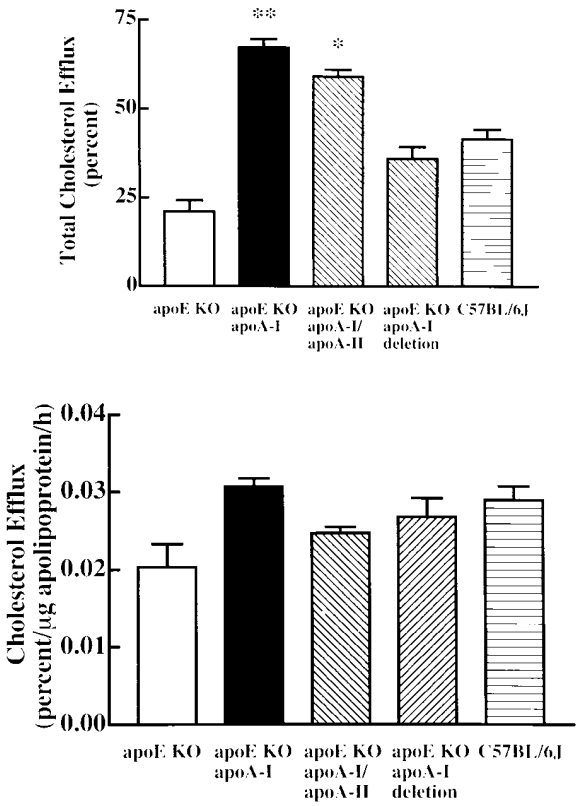

Figure 5. Cholesterol efflux. Total cholesterol efflux from lipid-loaded THP-1–derived macrophages by incubation with isolated HDL fractions of apo E KO mice, apo E KO mice overexpressing apo AI, the apo AI/apo AII chimera or the apo AI deletion mutant, and of C57BL/6J mice corresponding to 7.5% of serum HDL cholesterol (*top*). Fractional cholesterol efflux rates (*bottom*), expressed in percent cholesterol efflux/μg apolipoprotein/h, were calculated on the basis of the sum of human and murine apo AI amounts.

in which HDL remove excess cholesterol from peripheral cells and this cholesterol is then returned to the liver for excretion or for conversion to bile acids. The first step in this reverse cholesterol transport is the uptake of cellular cholesterol by lipoprotein acceptors in the interstitial fluid. Therefore, the capacity of HDL isolated from the plasma of apo E KO overexpressing the different human apo AI variants were compared with that of HDL of apo E KO mice. After incubation of lipid loaded THP-1–derived macrophages with HDL amounts corresponding to 7.5% of total serum HDL, the capacity to induce cholesterol efflux ranked: HDL of apo E KO mice $\leq$ HDL of des-(190-243)-apo AI/apo E KO mice $<<$ HDL of apo AI-(1-189)-apo AII-(12-77)/apo E KO mice $\sim$ HDL of apo AI/apo E KO mice. However, fractional cholesterol efflux rates, expressed in percent cholesterol efflux/μg apolipoprotein/h, for the different HDL particles were very similar. The ratios between human apo AI and murine apo AI in HDL of transgenic mice were different: HDL of apo AI/apo E KO mice $>$ HDL of apo AI-(1-189)-apo AII-(12-77)/apo E KO mice $>>$ HDL of des-(190-243)-apo AI/apo E KO mice. However, despite these differences in human to murine apolipoprotein ratios, the fractional cholesterol efflux rates for HDL of the different transgenic mice were not different and were also not different from those of HDL of apo E KO and C57BL/6J mice. These data suggest that the amino acid sequence of the carboxyl-terminal domain of human apo AI, apart from its ability to determine lipoprotein association, is not critical for the efficiency of HDL to act as cholesterol acceptors and that HDL of apo AI/apo E KO mice, despite their human-like distribution profile, were similar cholesterol acceptors as murine HDL, either derived from apo E KO or C57BL/6J mice. Previously, Atger et al. (25) have demonstrated that overexpression of human apo AI in the C57BL/6J background did not increase the cholesterol efflux potential of serum despite very significant increases of HDL cholesterol levels. It was concluded that the efficiency of HDL of human apo AI transgenic mice as cholesterol acceptors was lower than that of HDL of control mice. In this study, however, the increase of HDL cholesterol levels in apo E KO mice was associated with an increase in cholesterol efflux potential. Our data are thus in agreement with earlier findings of Francone et al. (26) and Castro et al. (27) that both isolated HDL and serum of human apo AI transgenic mice induced more cholesterol efflux than HDL or serum from apo E KO mice.

In summary, our data are thus in agreement with the proposed model in humans in which endogenous apo AI expression is an important determinant of the concentration of HDL, of the net efflux of cholesterol, and removal of excess cholesterol from peripheral foam cells and thus of the reverse cholesterol transport, and of the risk of atherosclerosis. Without affecting endogenous apolipoprotein production, deletion of the carboxyl-terminal domain of apo AI is associated with a decrease of HDL levels due to increased HDL turnover and thus with a decrease of the cholesterol efflux potential. The reduced cholesterol efflux potential of HDL of apo E KO mice overexpressing the deletion mutant is thus rather due to the deletion of a domain that determines HDL turnover than to the deletion of a domain that is critical for interaction with lipid-loaded cells. An important observation was that the amino acid sequence of apo AI was only marginally important for HDL metabolism, cholesterol efflux, and protection against atherosclerosis. Substitution of the carboxyl-terminal domain of apo AI with sequences of apo AII in such a way that the overall helical structure of the apolipoprotein was restored (19) restored also HDL turnover and cholesterol efflux. Although it has been demonstrated earlier that overexpression of murine apo AII in transgenic mice and of human apo AII in apo AI transgenic mice resulted in a reduction of the cholesterol efflux potential of their HDL and in an increase of the atherosclerosis susceptibility of these mice (15, 18), our data indicate that the apo AII amino acid sequence by itself does not affect HDL turnover, cholesterol efflux from lipid-loaded macrophages, and the protective effect of HDL against atherosclerosis. Interestingly, overexpression of the carboxyl-terminal deletion mutant of apo AI resulted in the generation of small HDL particles, which were also observed in transgenic mice overexpressing human apo AII (17), whereas overexpression of a chimeric molecule in which the helical sequences of apo AII are linked to the Asp1-Leu189 sequence of apo AI, resulting in restoring the molecular structure of apo AI, results in the generation of larger HDL particles and thus in a significant increase of HDL cholesterol levels. Although it has been suggested previously that increased atherosclerosis susceptibility of apo AI/apo AII transgenic mice compared with that of apo AI transgenic mice was due to differences in protein content of HDL (15, 28), it may thus also be due to differences in HDL distribution profile and HDL turnover. Our data indeed demonstrate that insertion of the apo AII sequence in the apo AI structure does not result in a molecule that is less antiatherogenic than apo AI and suggest that the helical distribution in apo AI is far more important for its role in HDL metabolism and protection against atherosclerosis than its amino acid sequence.

Thus this study demonstrates that although the tertiary structure of apo AI, e.g., number and organization of amphipathic helices especially in its carboxyl-terminal domain, is critical to produce HDL that protect better against atherosclerosis than apo AII containing HDL molecules, amino acid sequences of apo AII can be used to restore this optimal tertiary structure.

Acknowledgments

Ann Dhoest is a research assistant of the "Vlaams Instituut ter bevordering van het Wetenschappelijk-Technologisch Onderzoek in de Industrie." This work was supported by the Interuniversitaire Attractiepolen (Program 4/34) and by the Fonds voor Wetenschappelijk Onderzoek-Vlaanderen (Program G.3063.94).

References

1. Gordon, D.J., and B.M. Rifkind. 1989. High-density lipoprotein—the clinical implications of recent studies. *N. Engl. J. Med.* 321:1311–1316.

2. Assmann, G., and H.B. Brewer, Jr. 1974. Lipid-protein interactions in high density lipoproteins. *Proc. Natl. Acad. Sci. USA*. 71:989–993.

3. Schaefer, E.J., W.H. Heaton, M.G. Wetzel, and H.B. Brewer, Jr. 1982. Plasma apolipoprotein A-1 absence associated with a marked reduction of high density lipoproteins and premature coronary artery disease. *Arteriosclerosis.* 2: 16–26.

4. Walsh, A., Y. Ito, and J.L. Breslow. 1989. High levels of human apolipoprotein A-I in transgenic mice result in increased plasma levels of small high density lipoprotein (HDL) particles comparable to human HDL_3. *J. Biol. Chem.* 264:6488–6494.

5. Rubin, E.M., B.Y. Ishida, S.M. Clift, and R.M. Krauss. 1991. Expression of human apolipoprotein A-I in transgenic mice results in reduced plasma levels of murine apolipoprotein A-I and the appearance of two new high density lipoprotein size subclasses. *Proc. Natl. Acad. Sci. USA*. 88:434–438.

6. Holvoet, P., S. Danloy, and D. Collen. 1997. Role of the carboxy-terminal

domain of human apolipoprotein AI in high-density-lipoprotein metabolism—a study based on deletion and substitution variants in transgenic mice. *Eur. J. Biochem.* 245:642–647.

7. Hayek, T., Y. Ito, N. Azrolan, R.B. Verdery, K. Aalto Setala, A. Walsh, and J.L. Breslow. 1993. Dietary fat increases high density lipoprotein (HDL) levels both by increasing the transport rates and decreasing the fractional catabolic rates of HDL cholesterol ester and apolipoprotein (apo) A-I. Presentation of a new animal model and mechanistic studies in human apo A-I transgenic and control mice. *J. Clin. Invest.* 91:1665–1671.

8. Rubin, E.M., R.M. Krauss, E.A. Spangler, J.G. Verstuyft, and S.M. Clift. 1991. Inhibition of early atherogenesis in transgenic mice by human apolipoprotein AI. *Nature.* 353:265–267.

9. Plump, A.S., J.D. Smith, T. Hayek, K. Aalto Setala, A. Walsh, J.G. Verstuyft, E.M. Rubin, and J.L. Breslow. 1992. Severe hypercholesterolemia and atherosclerosis in apolipoprotein E-deficient mice created by homologous recombination in ES cells. *Cell.* 71:343–353.

10. Zhang, S.H., R.L. Reddick, J.A. Piedrahita, and N. Maeda. 1992. Spontaneous hypercholesterolemia and arterial lesions in mice lacking apolipoprotein E. *Science.* 258:468–471.

11. Nakashima, Y., A.S. Plump, E.W. Raines, J.L. Breslow, and R. Ross. 1994. ApoE-deficient mice develop lesions of all phases of atherosclerosis throughout the arterial tree. *Arterioscler. Thromb.* 14:133–140.

12. Reddick, R.L., S.H. Zhang, and N. Maeda. 1994. Atherosclerosis in mice lacking apo E. Evaluation of lesional development and progression. *Arterioscler. Thromb.* 14:141–147. [published erratum appears on 14:839]

13. Paszty, C., N. Maeda, J. Verstuyft, and E.M. Rubin. 1994. Apolipoprotein AI transgene corrects apolipoprotein E deficiency–induced atherosclerosis in mice. *J. Clin. Invest.* 94:899–903.

14. Plump, A.S., C.J. Scott, and J.L. Breslow. 1994. Human apolipoprotein A-I gene expression increases high density lipoprotein and suppresses atherosclerosis in the apolipoprotein E-deficient mouse. *Proc. Natl. Acad. Sci. USA.* 91:9607–9611.

15. Warden, C.H., C.C. Hedrick, J.H. Qiao, L.W. Castellani, and A.J. Lusis. 1993. Atherosclerosis in transgenic mice overexpressing apolipoprotein A-II. *Science.* 261:469–472. [published erratum appears on 262:164]

16. Schultz, J.R., E.L. Gong, M.R. McCall, A.V. Nichols, S.M. Clift, and E.M. Rubin. 1992. Expression of human apolipoprotein A-II and its effect on high density lipoproteins in transgenic mice. *J. Biol. Chem.* 267:21630–21636.

17. Marzal-Casacuberta, A., F. Blanco-Vaca, B.Y. Ishida, J. Julve Gil, J. Shen, S. Calvet-Marquez, F. Gonzalez-Sastre, and L. Chan. 1996. Functional lecithin:cholesterol acyltransferase deficiency and high density lipoprotein deficiency in transgenic mice overexpressing human apolipoprotein A-II. *J. Biol. Chem.* 271:6720–6728.

18. Schultz, J.R., J.G. Verstuyft, E.L. Gong, A.V. Nichols, and E.M. Rubin. 1993. Protein composition determines the anti-atherogenic properties of HDL in transgenic mice. *Nature.* 365:762–764.

19. Holvoet, P., Z. Zhao, E. Deridder, A. Dhoest, and D. Collen. 1996. Effects of deletion of the carboxyl-terminal domain of ApoA-I or of its substitution with helices of ApoA-II on in vitro and in vivo lipoprotein association. *J. Biol. Chem.* 271:19395–19401.

20. Bradford, M.M. 1976. A rapid and sensitive method for the quantitation of microgram quantities of protein using the principle of protein-dye binding. *Anal. Biochem.* 72:248–254.

21. Bolton, A.E., and W.M. Hunter. 1973. The use of antisera covalently coupled to agarose, cellulose and Sephadex in radioimmunoassay systems for proteins and haptens. *Biochim. Biophys. Acta.* 329:318–330.

22. Kleinberger, G., G. Heinzel, W. Druml, A. Laggner, and K. Lenz. 1987. Loading and maintenance dose for the determination of amino acid kinetics in plasma. *Infusionsther. Klin. Ernahr.* 1:40–44.

23. Tsuchiya, S., M. Yamabe, Y. Yamaguchi, Y. Kobayashi, T. Konno, and K. Tada. 1980. Establishment and characterization of a human acute monocytic leukemia cell line (THP-1). *Int. J. Cancer.* 26:171–176.

24. Holvoet, P., G. Perez, H. Bernar, E. Brouwers, B. Vanloo, M. Rosseneu, and D. Collen. 1994. Stimulation with a monoclonal antibody (mAb4E4) of scavenger receptor-mediated uptake of chemically modified low density lipoproteins by THP-1-derived macrophages enhances foam cell generation. *J. Clin. Invest.* 93:89–98.

25. Atger, V., M. de la Llera Moya, M. Bamberger, O. Francone, P. Cosgrove, A. Tall, A. Walsh, N. Moatti, and G. Rothblat. 1995. Cholesterol efflux potential of sera from mice expressing human cholesteryl ester transfer protein and/or human apolipoprotein AI. *J. Clin. Invest.* 96:2613–2622.

26. Francone, O.L., L. Royer, and M. Haghpassand. 1996. Increased prebeta-HDL levels, cholesterol efflux, and LCAT-mediated esterification in mice expressing the human cholesteryl ester transfer protein (CETP) and human apolipoprotein A-I (apoA-I) transgenes. *J. Lipid Res.* 37:1268–1277.

27. Castro, G., L.P. Nihoul, C. Dengremont, C. de Geitere, B. Delfly, A. Tailleux, C. Fievet, N. Duverger, P. Denefle, J.C. Fruchart, and E.M. Rubin. 1997. Cholesterol efflux, lecithin-cholesterol acyltransferase activity, and prebeta particle formation by serum from human apolipoprotein A-I and apolipoprotein A-I/apolipoprotein A-II transgenic mice consistent with the latter being less effective for reverse cholesterol transport. *Biochemistry.* 36:2243–2249.

28. Gong, E.L., L.J. Stolzfus, C.M. Brion, D. Murugesh, and E.M. Rubin. 1996. Contrasting in vivo effects of murine and human apolipoprotein A-II. *J. Biol. Chem.* 271:5984–5987.